Journal of Magnetic Resonance 307 (2019) 106571

Contents lists available at ScienceDirect

Journal of Magnetic Resonance

journal homepage: www.elsevier.com/locate/jmr

Nonlinear sampling in ultrafast Laplace NMR

Vladimir V. Zhivonitko, Md Sharif Ullah, Ville-Veikko Telkki *

NMR Research Unit, University of Oulu, P.O. Box 3000, 90014 Oulu, Finland

ARTICLE INFO

Article history:
Received 25 June 2019
Revised 9 August 2019
Accepted 9 August 2019
Available online 13 August 2019

Keywords:
Laplace NMR
NMR relaxation
Non-uniform sampling
Ultrafast NMR

ABSTRACT

Ultrafast Laplace NMR (UF-LNMR) reduces the experiment time of multidimensional relaxation and diffusion measurements to a fraction. Here, we demonstrate a method for nonlinear (in this case logarithmic) sampling of the indirect dimension in UF-LNMR measurements. The method is based on the use of frequency-swept pulses with the frequency nonlinearly increasing with time. This leads to an optimized detection of exponential experimental data and significantly improved resolution of LNMR parameters.

1. Introduction

NMR relaxation and diffusion experiments provide detailed information about molecular rotational and translational motion as well as chemical resolution complementary to frequency spectra [1–3]. The experiments result in exponentially decaying or increasing data, and the distribution of relaxation times or diffusion coefficients is solved by the inverse Laplace transform [4]. Therefore, the relaxation and diffusion experiments are called Laplace NMR.

Like in traditional NMR spectroscopy, the resolution and information content of LNMR can be increased substantially by a multidimensional approach [1–3]. However, the approach leads to very long experiment times due to need for repetitions with an incremented evolution time or gradient strength. Furthermore, the need for repetitions significantly hinders the use of modern hyperpolarization methods [5–8], which otherwise could improve the experimental sensitivity up to five orders of magnitude.

Recently, we have shown that the experiment time of multidimensional LNMR can be shortened by one to three orders of magnitude by encoding the incremented variables of an indirect dimension into the layers of the sample [9–15]. The method is called ultrafast LNMR, and it has found diverse applications in the investigation of porous media, chemical analysis, identification of intra- and extracellular metabolites as well as low-field, mobile NMR [9–15]. The single-scan approach also facilitates significantly the use of hyperpolarization to boost sensitivity. Originally, the spatial encoding was exploited in ultrafast NMR spectroscopy [16–20], and the principles have also been exploited in single-scan inversion recovery T_1 measurements [21,22] as well as diffusion ordered spectroscopy (DOSY) [23–26].

In this communication, we describe a method for nonlinear sampling of the indirect dimension in UF-LNMR experiments. This leads to an optimized detection of the exponential experimental data and significantly improved resolution of LNMR parameters.

2. Methods

If an observable, which is exponentially dependent on time, is sampled with a constant time step (linear sampling), then the beginning of the data is sampled in a non-optimal way, as the change of the observable is the biggest in the beginning. If the data is a sum of several exponential components, the situation is even worse; in the extreme case, the fastest changing component is not sampled at all. In traditional LNMR experiments, this problem is overcome by using a logarithmic sampling, *i.e.*, by keeping the difference of natural logarithms of successive sampling point times constant. Consequently, the rapidly changing initial part of the data is more densely sampled, leading to more optimal detection of both single- and multi-exponential data. [27]

In all the UF-LNMR experiments based on continuous spatial encoding, the spatial encoding is realized by applying an adiabatic frequency-swept pulse with frequency linearly increasing (or decreasing) with time along with a magnetic field gradient [9–26]. This leads to a linear (non-optimal) sampling of the indirect dimension; the evolution time τ or spatial frequency q is linearly increasing (or decreasing) with the position.

For example, the pulse sequence for UF T_1-T_2 correlation experiment is shown in Fig. 1a [9]. The initial magnetic field gradient pulse G_{se} makes the Larmor frequency of nuclei linearly dependent

* Corresponding author.
E-mail address: ville-veikko.telkki@oulu.fi (V.-V. Telkki).

https://doi.org/10.1016/j.jmr.2019.106571
1090-7807/

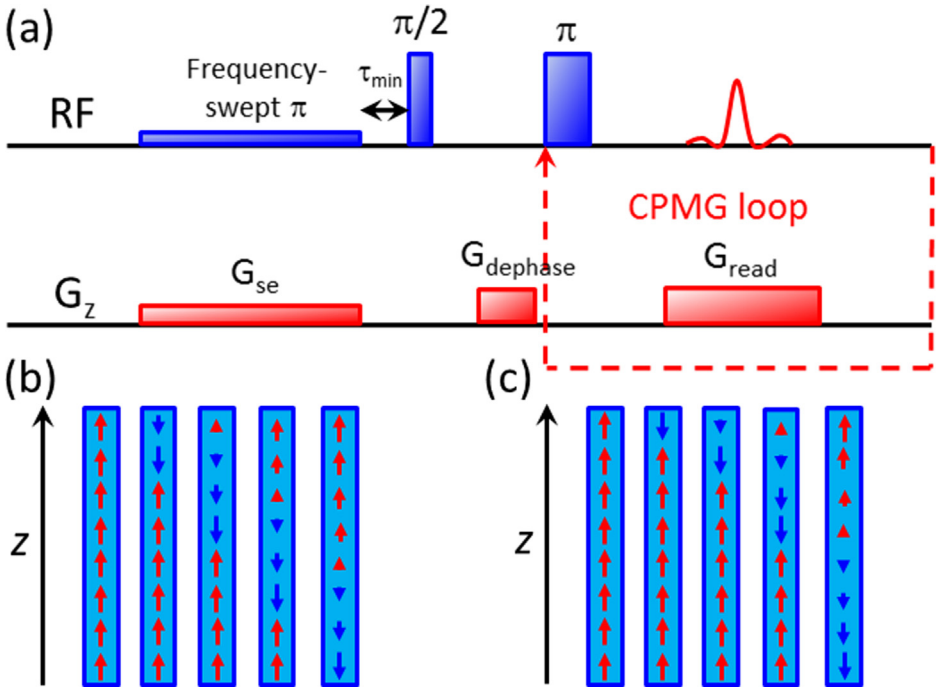

Fig. 1. (a) The pulse sequence for ultrafast T_1-T_2 correlation experiment. Magnetisation vectors at different layers of a sample during spatial encoding using (b) linear and (c) nonlinear frequency sweep.

on position. If a frequency-swept π pulse with the frequency linearly decreasing with time is applied together with the gradient, the spins in top of the sample tube are inverted first and those in bottom last, as visualized in Fig. 1b. The inversion time is linearly dependent on position. At the end of the pulses, the spins in the top have almost fully recovered back to the thermal equilibrium, and the magnetization profile along the z axis corresponds to the traditional inversion recovery curve. The profile is read in the CPMG loop by using a read gradient like in magnetic resonance imaging (MRI). Because the recovery time is linearly dependent on the position, the approach leads to linearly sampled T_1 data.

A simple way to change from the linear to logarithmic sampling of the indirect dimension in UF-LNMR experiments is to make the frequency sweep nonlinear. For example, in the UF T_1-T_2 correlation experiment, the frequency of the adiabatic pulse, ν_F, should vary logarithmically with time t (see Section 3 in Supporting Information):

$$\nu_F = \Delta\nu \left[\frac{\ln\left[\frac{1}{2}(\tau_{max}+\tau_{min}) - (\tau_{max}-\tau_{min})\frac{t}{t_F}\right] - \ln(\tau_{max})}{\ln(\tau_{max}) - \ln(\tau_{min})} + \frac{1}{2} \right] \quad (1)$$

Here, $\Delta\nu = \nu_i - \nu_f$ is the width of the frequency sweep, ν_i and ν_f are the initial and final frequencies of the sweep, τ_{min} and τ_{max} are the minimum (see Fig. 1a) and maximum recovery times, $t_F = \tau_{max} - \tau_{min}$ is the length of the frequency-swept π pulse, and $-t_F/2 \le t \le +t_F/2$. Consequently, the recovery time τ is exponentially increasing with position z (see Section 3 in Supporting Information):

$$\tau = \exp\left\{ [\ln(\tau_{max}) - \ln(\tau_{min})] \left(\frac{\gamma G z}{2\pi\Delta\nu} - \frac{1}{2} \right) + \ln(\tau_{max}) \right\}. \quad (2)$$

Here, γ is the gyromagnetic ratio, G is the gradient strength, and the spatial encoding region is $-\pi\Delta\nu/\gamma G \le z \le +\pi\Delta\nu/\gamma G$.

This analysis is based on the instantaneous inversion approximation, *i.e.*, we assume that the spins in certain layer are inverted instantaneously when their Larmor frequency matches with the frequency of the adiabatic pulse. This has turned out to be a good approximation [18]. The power of the adiabatic pulse has to be high enough so that the adiabatic condition is satisfied even at the end of the pulse, when the sweep rate is fastest (once the power is high enough, the adiabatic pulse is inverting the magnetization independently of the pulse power) [18]. Alternatively, the amplitude of the frequency-swept pulse may increase with time to fulfil the adiabatic condition. The validity and limitations of instantaneous excitation and inversion as well as adiabatic condition are discussed in detail elsewhere [28].

3. Results and discussion

To validate that the nonlinear sampling method works, we performed UF inversion recovery (UF-IR) measurements of single- and double-tube water samples visualized in Fig. 2a. The experiments were performed with Bruker Avance III 400 MHz spectrometer (see experimental details in Section 1 in Supporting Information). Water was doped with copper chlorite so that, according to the traditional IR reference measurements, T_1 in the inner compartment of the double-tube sample was about ten times longer (332 ± 2 ms) than in the outer compartment as well as in the single-tube sample (33.5 ± 0.2 ms). The UF-IR pulse sequence was otherwise identical to the UF T_1-T_2 correlation shown in Fig. 1a except that only one echo was measured in the CPMG loop. A frequency-swept π pulse with the pulse length t_F of 1 s and frequency nonlinearly increasing from −5000 to +5000 Hz (see Fig. 2b) was used in the experiment for the spatial encoding. For comparison, linearly sampled data was also measured with a similar frequency-swept pulse with frequency linearly increasing with time (shown also in Fig. 2b; for more details of the pulse, see Section 2 in Supporting Information).

The magnetization profiles (*i.e.* the Fourier transforms of the UF-IR data sets in magnitude) of the single-tube sample are shown in Fig. 2c. The spatially encoded IR curves are visible in the sweep region indicated in the figure. In the case of the nonlinear sweep,

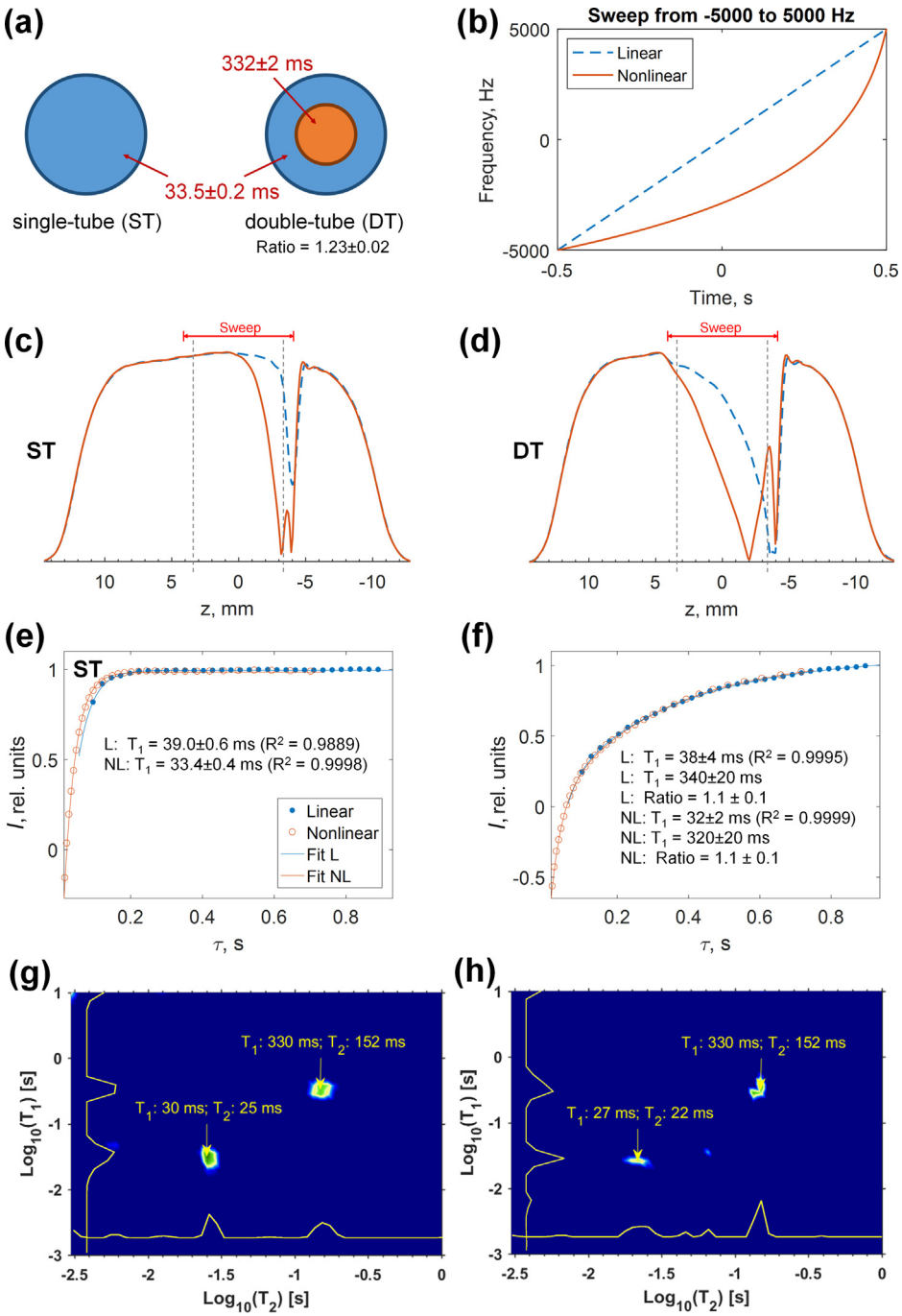

Fig. 2. (a) Illustrations of the single- and double-tube water samples doped with copper chloride. The values of T_1 times as well as the ratio of amplitudes of low (33.5 ms) to high (332 ms) relaxation time components in the double-tube sample are indicated in the figure. (b) Frequency sweeps used in linearly and nonlinearly sampled UF-IR experiments. Magnetization profiles of the single-(c) and double-tube (d) samples. The sweep range and the range of the data used in the T_1 analysis are indicated by red horizontal bar and grey vertical dashed lines, respectively. The IR curves for the single-(e) and double-tube (f) sample. The least squares fits of exponential functions (solid lines), along with the resulting T_1 values (standard deviation values given as errors) are also shown in the figures. Ultrafast T_1-T_2 correlation maps of the double-tube sample measured using the linear (g) and nonlinear (h) sampling. T_1 and T_2 projection traces are shown at the left and bottom edges of the images. (For interpretation of the references to colour in this figure legend, the reader is referred to the web version of this article.)

the minimum around $z = -3$ mm corresponds to the zero intensity of the IR curve. The other minimum around $z = -4$ mm is an artefact, because the adiabatic pulse does not work perfectly right in the beginning and end of the frequency sweep [18]. The linearly sampled data does not reach zero intensity at all, because the shortest recovery delays are not observed. The magnetization profiles of the double tube sample in Fig. 2d show also that the IR curve is much better probed in the case of the nonlinear sweep.

Fig. 2e and f show the ultrafast IR curves extracted from the magnetization profiles. In the processing, the profiles were subjected to the coil sensitivity profile correction and the data close to the beginning and end of the frequency sweep were removed [9]. Then the position axis z was converted into recovery time axis τ by using Eqs. (S5) and (S23) shown in Supporting information for the linearly and nonlinearly sampled data, respectively. The figures visualize clearly much more optimal sampling of the IR curves with

nonlinear sweep than with linear; much shorter recovery times are observed and therefore the beginning part of the IR curve is much better sampled. The observed recovery times varied from 102 to 910 ms and from 18 to 747 ms for the linear and nonlinear sweep, respectively. The T_1 values resulted from single- or double-exponential fits shown in the figures are in good agreement with the reference experiments within the error bars, while in the case of linear sampling the deviations are bit larger (see also difference traces between the data and fits in Fig. S9 in Supporting Information).

We performed also full T_1-T_2 correlation experiments for the double-tube sample using the pulse sequence shown in Fig. 1a. The correlation maps resulting from the 2D Laplace inversion [29,30] of the data measured using linear and nonlinear sweep are visible in Fig. 2g and 2h, respectively. Both maps show two components corresponding to the two compartments, and they are in a good mutual agreement, proving that the nonlinear sampling concept works also in 2D LNMR experiments. In the nonlinear map, the low relaxation time signal is about 40% narrower in the T_1 dimension than in the linear map due to the more optimal sampling (see Fig. S10 in Supporting Information), resulting in improved resolution of the components (note that the line widths depend also on the parameters used in the Laplace inversion).

As a final demonstration of the feasibility of the nonlinear ultrafast sampling, we measured ultrafast and reference T_1-T_2 correlation maps of water in Silica gel 60 porous material. The results are shown in Fig. 3. All the maps show two dominant peaks, one from water inside the pores (nominal pore size 60 Å) characterized by the shorter relaxation times and another from bulk water in between the particles (particle size 63–200 μm) of the porous material. However, in the UF-linear map the signals are in a significantly narrower region in the T_1 dimension than in the other maps due to the non-optimal sampling. Furthermore, in the UF-nonlinear map the signals are in a slightly narrower region in the T_1 dimension than in the normal reference map. Most probably, this is a consequence of the effect of magnetic field inhomogeneity in the porous material on the spatial encoding. The linewidth of the water in porous material is about 110 Hz, which is a significant portion of the frequency range (30 kHz) used in the spatial encoding. Therefore, a certain point in the observed magnetization profile does not anymore correspond to a single recovery delay, but it represents contributions of a range of delays. This leads to an averaging effect; a narrower range of T_1 values is observed. The averaging effect might be reduced by using larger gradient amplitude and sweep width in the spatial encoding.

Regardless of the above mentioned issues, the two water sites are visible in the ultrafast maps, and T_2 range as well as the average values of T_1 are in good agreement with the reference map. In fact, the coordinates of the tops of the peaks in the non-linearly sampled ultrafast and reference maps are close to each other, and, if the peak widths are taken as experimental error, the maps can be considered to be in good agreement with each other.

As the T_1 values of the components observed from the Silica sample are much longer than the T_2 values, the diffusion driven exchange of water between the pore and bulk sites has more significant averaging effect on the T_1 than T_2 values. On the other hand, the effect of exchange should be the same for the ultrafast and reference experiments, as the both types of experiments rely on the observation of similar exponential data.

It is noteworthy that the ultrafast experiments with 4 accumulated scans took only for 30 s while the reference experiment with the same number of scans lasted for 16 min. Naturally, the signal-to-noise ratio (SNR) in the ultrafast experiments was lower than in the reference experiment due to splitting the sample into layers in the spatial encoding. However, the observed SNR decreases have been relatively small (factors of 2–4), which is not a problem with

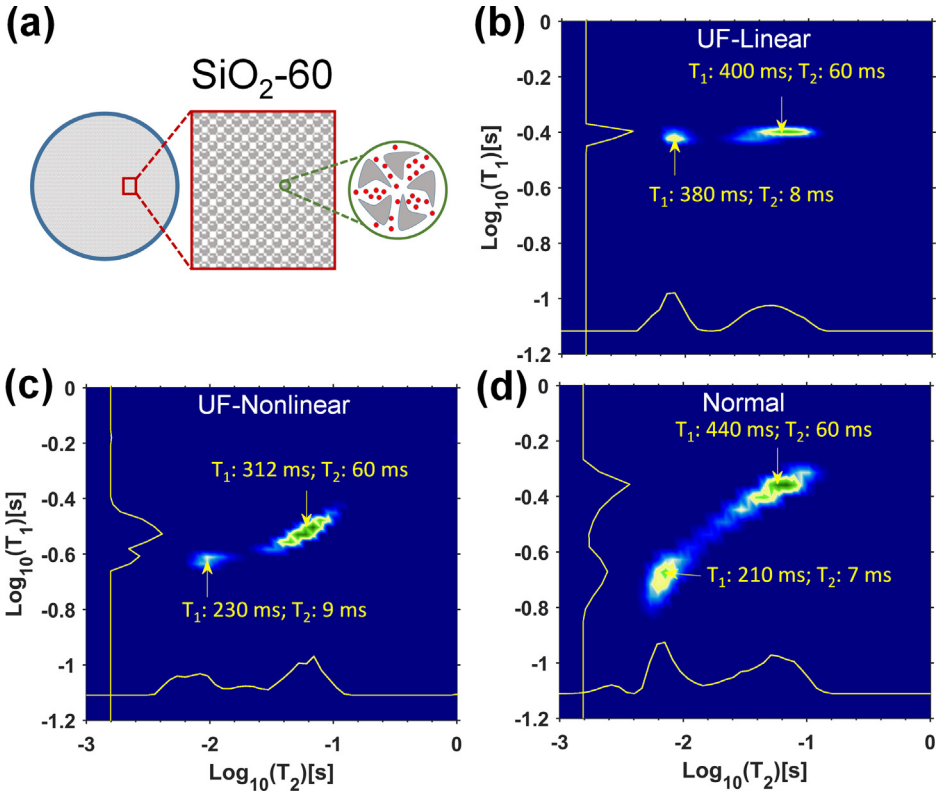

Fig. 3. (a) Illustrations of the porous material sample including Silica gel 60 immersed in water doped by copper chloride. Ultrafast T_1-T_2 correlation maps measured using the (b) linear and (c) nonlinear sampling. (d) Corresponding map measured using the traditional reference experiment. T_1 and T_2 projection traces are shown at the left and bottom edges of the images.

the high concentration samples, and the ultrafast experiment can be repeated several times during a single traditional experiment, which may lead to even improved SNR per unit time [10,13]. Furthermore, the single-scan approach makes it possible to increase the sensitivity by several orders of magnitude by hyperpolarization [10–12,14].

4. Conclusions

We demonstrated a method for nonlinear sampling of indirect dimension in the UF IR and T_1-T_2 correlation experiments. The method is based on the use of frequency-swept pulses with the frequency nonlinearly increasing with time. This leads to more optimal detection of single-exponential data and much more optimal detection of multi-exponential data with T_1 values differing significantly. Therefore, it results in significantly improved resolution of T_1 distribution. The maximum T_1 value observable in the ultrafast experiments is defined by the length of the frequency-swept pulse used in spatial encoding, and there is no fundamental technical limitation for the length. As shown in this Communication, much shorter T_1 values can be observed by using the non-linear sampling instead of the linear. Adiabatic condition and instantaneous excitation approximation sets additional limits for the minimum observable T_1 value [18,28]. Here, we focused on logarithmic sampling, but other kinds of non-linear sampling schemes can be readily obtained with appropriate modifications of the sweep function of the frequency-swept pulse. The method can be extended to many other multidimensional ultrafast Laplace NMR experiments including indirect T_1 encoding or experiments correlating T_1 with spectroscopic data [21,22]. Furthermore, it can be utilized for nonlinear sampling of spatial frequency (q) space in ultrafast diffusion experiments as well as other multidimensional ultrafast NMR experiments including indirect diffusion encoding [9–20]. The optimized multidimensional UF-LNMR experiments have lots of interesting potential applications in various disciplines, including chemistry, biochemistry, geology, archaeology, and medicine [1–3,9–15,31–35].

Acknowledgement

We acknowledge the financial support of the European Research Council (ERC) under Horizon 2020 (H2020/2018-2022/ERC grant agreement no. 772110), Academy of Finland (grants #289649, 294027, 319216 and 323480), the Kvantum institute (University of Oulu), and the COST action CA15209 “European Network on NMR Relaxometry. The Laplace inversion program was provided by the group of late Prof. P. Callaghan.

Appendix A. Supplementary material

Supplementary data to this article can be found online at https://doi.org/10.1016/j.jmr.2019.106571.

References

[1] P.T. Callaghan, Translational Dynamics and Magnetic Resonance: Principles of Pulsed Gradient Spin Echo NMR, Oxford University Press, Oxford; New York, 2011.
[2] D. Bernin, D. Topgaard, NMR diffusion and relaxation correlation methods: new insights in heterogeneous materials, Curr. Opin. Colloid. In. 18 (2013) 166–172.
[3] Y.Q. Song, Magnetic Resonance of Porous Media (MRPM): a perspective, J. Magn. Reson. 229 (2013) 12–24.
[4] V.-V. Telkki, Hyperpolarized Laplace NMR, Magn. Reson. Chem. 56 (2018) 619–632.
[5] J.H. Ardenkjaer-Larsen, B. Fridlund, A. Gram, G. Hansson, L. Hansson, M.H. Lerche, R. Servin, M. Thaning, K. Golman, Increase in signal-to-noise ratio of >10,000 times in liquid-state NMR, Proc. Natl. Acad. Sci. USA 100 (2003) 10158–10163.
[6] C.R. Bowers, Sensitivity enhancement utilizing parahydrogen, in: D.M. Grant, R.K. Harris (Eds.), Encyclopedia of Nuclear Magnetic Resonance, Wiley, Chichester, 2002, pp. 750–769.
[7] R.W. Adams, J.A. Aguilar, K.D. Atkinson, M.J. Cowley, P.I. Elliott, S.B. Duckett, G. G. Green, I.G. Khazal, J. Lopez-Serrano, D.C. Williamson, Reversible interactions with para-hydrogen enhance NMR sensitivity by polarization transfer, Science 323 (2009) 1708–1711.
[8] D.A. Barskiy, A.M. Coffey, P. Nikolaou, D.M. Mikhaylov, B.M. Goodson, R.T. Branca, G.J. Lu, M.G. Shapiro, V.-V. Telkki, V.V. Zhivonitko, I.V. Koptyug, O.G. Salnikov, K.V. Kovtunov, V.I. Bukhtiyarov, M.S. Rosen, M.J. Barlow, S. Safavi, I.P. Hall, L. Schröder, E.Y. Chekmenev, NMR hyperpolarization techniques of gases, Chem. Eur. J. 23 (2017) 725–751.
[9] S. Ahola, V.V. Telkki, Ultrafast two-dimensional NMR relaxometry for investigating molecular processes in real time, ChemPhysChem 15 (2014) 1687–1692.
[10] S. Ahola, V.V. Zhivonitko, O. Mankinen, G. Zhang, A.M. Kantola, H.-Y. Chen, C. Hilty, I.V. Koptyug, V.-V. Telkki, Ultrafast multidimensional laplace NMR for a rapid and sensitive chemical analysis, Nat. Commun. 6 (2015) 8363.
[11] O. Mankinen, J. Hollenbach, S. Ahola, J. Matysik, V.-V. Telkki, Ultrafast Laplace NMR with hyperpolarized xenon gas, Micropor. Mesopor. Mater. 269 (2018) 75–78.
[12] G. Zhang, S. Ahola, M.H. Lerche, V.-V. Telkki, C. Hilty, Identification of intracellular and extracellular metabolites in cancer cells using 13C hyperpolarized ultrafast Laplace NMR, Anal. Chem. 90 (2018) 11131–11137.
[13] J.N. King, V.J. Lee, S. Ahola, V.-V. Telkki, T. Meldrum, Ultrafast multidimensional Laplace NMR using a single-sided magnet, Angew. Chem. Int. Ed. 55 (2016) 5040–5043.
[14] J.N. King, A. Fallorina, J. Yu, G. Zhang, V.-V. Telkki, C. Hilty, T. Meldrum, Probing molecular dynamics with hyperpolarized ultrafast Laplace NMR using a low-field, single-sided magnet, Chem. Sci. 9 (2018) 6143–6149.
[15] L. Venturi, J. Warner, B. Hills, Multisliced ultrafast 2D relaxometry, Magn. Reson. Imag. 28 (2010) 964–970.
[16] L. Frydman, T. Scherf, A. Lupulescu, The acquisition of multidimensional NMR spectra within a single scan, Proc. Natl. Acad. Sci. USA 99 (2002) 15858–15862.
[17] P. Pelupessy, Adiabatic single scan two-dimensional NMR spectrocopy, J. Am. Chem. Soc. 125 (2003) 12345–12350.
[18] A. Tal, L. Frydman, Single-scan multidimensional magnetic resonance, Prog. Nucl. Magn. Reson. Spectrosc. 57 (2010) 241–292.
[19] P. Giraudeau, L. Frydman, Ultrafast 2D NMR: an emerging tool in analytical spectroscopy, Annu. Rev. Anal. Chem. (2014) 129–161.
[20] B. Gouilleux, B. Charrier, S. Akoka, F.X. Felpin, M. Rodriguez-Zubiri, P. Giraudeau, Ultrafast 2D NMR on a benchtop spectrometer: applications and perspectives, TrAC-Trend. Anal. Chem. 83 (2016) 65–75.
[21] N.M. Loening, M.J. Thrippleton, J. Keeler, R.G. Griffin, Single-scan longitudinal relaxation measurements in high-resolution NMR spectroscopy, J. Magn. Reson. 164 (2003) 321–328.
[22] P.E.S. Smith, K.J. Donovan, O. Szekely, M. Baias, L. Frydman, Ultrafast NMR T1 relaxation measurements: probing molecular properties in real time, ChemPhysChem 14 (2013) 3138–3145.
[23] M.J. Thrippleton, N.M. Loening, J. Keeler, A fast method for the measurement of diffusion coefficients: one-dimensional DOSY, Magn. Reson. Chem. 41 (2003) 441–447.
[24] Y. Shrot, L. Frydman, Single-scan 2D DOSY NMR spectroscopy, J. Magn. Reson. 195 (2008) 226–231.
[25] L. Guduff, D. Kurzbach, C. van Heijenoort, D. Abergel, J.N. Dumez, Single-scan C-13 diffusion-ordered NMR spectroscopy of DNP-hyperpolarised substrates, Chem. Eur. J. 23 (2017) 16722–16727.
[26] L. Guduff, I. Kuprov, C. van Heijenoort, J.N. Dumez, Spatially encoded 2D and 3D diffusion-ordered NMR spectroscopy, Chem. Commun. 53 (2017) 701–704.
[27] Y.-Q. Song, L. Venkataramanan, L. Burcaw, Determining the resolution of Laplace inversion spectrum, J. Chem. Phys. 122 (2005) 104104.
[28] V.-V. Telkki and Vladimir V. Zhivonitko, Ultrafast NMR diffusion and relaxation studies, Annu. R. NMR S., 97, 2019, 83-119.
[29] L. Venkataramanan, Y.Q. Song, M.D. Hürlimann, Solving Fredholm integrals of the first kind with tensor product structure in 2 and 2.5 dimensions, IEEE Trans. Signal Process. 50 (2002) 1017–1026.
[30] Y.Q. Song, L. Venkataramanan, M.D. Hürlimann, M. Flaum, P. Frulla, C. Straley, T_1–T_2 correlation spectra obtained using a fast two-dimensional Laplace inversion, J. Magn. Reson. 154 (2002) 261–268.
[31] B. Blümich, J. Perlo, F. Casanova, Mobile single-sided NMR, Prog. Nucl. Magn. Reson. Spectrosc. 52 (2008) 197–269.
[32] D. Kruk, A. Herrmann, E.A. Rossler, Field-cycling NMR relaxometry of viscous liquids and polymers, Prog. Nucl. Magn. Reson. Spectrosc. 63 (2012) 33–64.
[33] M. Akke, Conformational dynamics and thermodynamics of protein-ligand binding studied by NMR relaxation, Biochem. Soc. Trans. 40 (2012) 419–423.
[34] L. Avram, Y. Cohen, Diffusion NMR of molecular cages and capsules, Chem. Soc. Rev. 44 (2015) 586–602.
[35] M.A. Javed, S. Ahola, P. Håkansson, O. Mankinen, M.K. Aslam, A. Filippov, F.U. Shah, S. Glavatskih, O.N. Antzutkin, V.V. Telkki, Structure and dynamics elucidation of ionic liquids using multidimensional Laplace NMR, Chem. Commun. 53 (2017) 11056–11059.